Speciation Study of Chromium Corrosion Products in Molten LiF-NaF-KF Salt (Postprint)

Authors: Qiu Jie, ZOU Yang, YU Guo-Jun, Shang-Ming He, LIU Wen-Guan, JIA Yan-Yan, LI Zhi-Jun, XU Hong-Jie

Date: 2023-06-18T00:00:00+00:00

Abstract

To investigate the corrosion products of Cr in molten FLiNaK salt (46.5 mol% LiF–11.5 mol% NaF–42 mol% KF), the corrosion test of the pure metal Cr was performed in molten FLiNaK salt at 700 ℃ for 200 h. The FLiNaK salt after the corrosion test was thoroughly investigated by X-ray absorption near-edge structure spectroscopy, a transmission electron microscope, and X-ray diffraction. The results demonstrate that the predominant oxidation state of Cr in FLiNaK salt is Cr3+, and the main corrosion product in cooled FLiNaK salt is K2NaCrF6.

Full Text

Preamble

Speciation Study of Chromium Corrosion Product in Molten LiF-NaF-KF Salt

QIU Jie,[1],[2] ZOU Yang,[1] YU Guo-Jun,[1] HE Shang-Ming,[1] LIU Wen-Guan,[1] JIA Yan-Yan,[1] LI Zhi-Jun,[1] and XU Hong-Jie[1],†

[1]Shanghai Institute of Applied Physics, Chinese Academy of Sciences, Shanghai 201800, China
[2]University of Chinese Academy of Sciences, Beijing 100049, China

(Received January 28, 2015; accepted in revised form July 1, 2015; published online December 20, 2015)

Abstract: To investigate the corrosion products of Cr in molten FLiNaK salt (46.5 mol% LiF–11.5 mol% NaF–42 mol% KF), a corrosion test of pure metallic Cr was performed in molten FLiNaK salt at 700 °C for 200 h. The FLiNaK salt after the corrosion test was thoroughly investigated by X-ray absorption near-edge structure spectroscopy, transmission electron microscopy, and X-ray

diffraction. The results demonstrate that the predominant oxidation state of Cr in FLiNaK salt is Cr^{3+}, and the main corrosion product in cooled FLiNaK salt is K_2NaCrF_6.

Keywords: FLiNaK, Cr, Corrosion product, K_2NaCrF_6
DOI: 10.13538/j.1001-8042/nst.26.060602

Introduction

Among the reactor systems proposed in the Generation-IV International Forum, the molten salt reactor (MSR) has attracted considerable attention due to its unique features, such as high thermodynamic efficiency, intrinsic safety, and online refueling [1–4]. In MSRs, molten salt mixtures serve as the primary coolant or even as the fuel itself. These salts are characterized by high volumetric heat capacities, low viscosities, high boiling points, and other desirable properties [5]. However, molten salts are highly corrosive, especially at elevated temperatures, and corrosion of structural materials in molten salt environments represents one of the primary challenges preventing long-term MSR operation [1]. Consequently, extensive research has been conducted in recent years to investigate corrosion mechanisms of materials in molten salt environments [6–13].

It has been observed that among all candidate structural materials for MSRs, chromium is selectively attacked by molten fluoride salts, with corrosion rates correlating with the Cr content of the alloys [6, 7]. Despite this known susceptibility to selective attack, Cr remains widely used in high-temperature alloys because it enhances high-temperature oxidation resistance. Pure eutectic FLiNaK salt is emerging as a leading candidate for use as a secondary coolant in MSRs due to its advantageous thermal and physical properties [5, 14]. Therefore, a systematic study of the corrosion mechanism of Cr in molten FLiNaK salt is essential to ensure its safe application in MSRs.

To achieve this understanding, it is necessary to identify the corrosion products of Cr in molten FLiNaK salts. However, to our knowledge, most previous research has focused on corrosion products of Cr in fluoride fuel salts and/or nitrates [14–16], where uranium plays a key role in the corrosion process. While a good understanding of fuel salt corrosion has been developed, few data are available for pure coolant salts such as FLiNaK. Consequently, precise identification of Cr corrosion products in pure FLiNaK salt is highly desirable. Since the Cr content of most high-temperature alloys does not exceed 25 wt.%, pure metallic Cr was selected for this study to yield sufficient concentrations of corrosion products for identification. In this work, metallic Cr was exposed to molten FLiNaK salt in a graphite crucible at 700 °C for 200 h. After the corrosion test, the FLiNaK salt was investigated using X-ray absorption near-edge structure spectroscopy (XANES), transmission electron microscopy (TEM), and X-ray diffraction (XRD). The results show that the main corrosion product of Cr in FLiNaK salt is K_2NaCrF_6.

II. Experiment

The pure FLiNaK eutectic salt was supplied by the Shanghai Institute of Organic Chemistry, Chinese Academy of Sciences. The impurities in the salt, as detected by inductively coupled plasma-optical emission spectrometry (ICP-OES), were as follows: 6 ppm Fe, 74 ppm Ni, 1 ppm Cr, 11 ppm Ca, 17 ppm Mg, 8 ppm Zn, and 6 ppm P. The water content was less than 100 ppm as determined using a Karl Fischer water analyzer. High-purity Cr was purchased from Beijing Cuibolin Non-ferrous Technology Developing Co., Ltd. The metal Cr used in this work consisted of irregular pieces with a purity of 99.99%.

The corrosion test was performed in a graphite crucible due to the relative inertness of graphite to molten fluoride salts [6, 17]. The crucible was fabricated from purified graphite (CDI-1A). Prior to the corrosion test, the graphite crucible was ultrasonically cleaned in ethanol and then baked at 800 °C for 12 h under vacuum to remove contaminants, residual oxygen, and water. After heat treatment, the crucible was removed from the furnace and immediately stored in an argon-atmosphere glove box. Subsequently, 30 g of pure Cr pieces and 120 g of FLiNaK salt were placed in the graphite crucible. To ensure salt purity, the graphite crucible was sealed in a 316 stainless steel capsule and welded shut in the argon-atmosphere glove box. The schematic diagram of the corrosion test capsule is shown in Fig. 1 [FIGURE:1].

After final welding, the capsule was transferred to a furnace and heated at 700 °C for 200 h. Following the corrosion test, the capsule was cooled to room temperature and sliced open on a lathe. The Cr concentration in the FLiNaK salt after corrosion testing was analyzed by ICP-OES. Corrosion products were identified by XANES, TEM (FEI Tecnai G2 F20, 200 kV), and XRD (Rigaku D/max2500 V, Cu Kα, $\lambda = 0.154$ nm). The TEM sample was ultrasonically dispersed in ethanol and transferred to a carbon-coated copper TEM grid. Cr K-edge XANES spectra in fluorescence yield mode were measured at the BL14W1 beamline of the Shanghai Synchrotron Radiation Facility (SSRF) [18], which operates at an energy of up to 3.5 GeV and a stored current of 240 mA. The energy scale of the XANES spectra for the Cr K-edge (5.989 keV) was calibrated using a Cr metal foil. To avoid oxygen contamination of the retrieved FLiNaK salt, all salt samples were sealed in plastic bags during XANES and XRD analyses.

III. Results and Discussion

The cooled FLiNaK salt was retrieved after the corrosion test at 700 °C for 200 h. As shown in Fig. 2, the color of the FLiNaK salt changed from white to black-green after the corrosion test, primarily due to Cr dissolution [19]. According to ICP-OES analysis, the Cr and Ni contents in the FLiNaK salt after corrosion testing were (2403 $\pm$ 190) ppm and (4.4 $\pm$ 0.2) ppm, respectively. The Fe concentration was below the quantitative detection limits of ICP-OES, as shown in Table 1. The Ni and Fe contents in the salt after corrosion testing were lower than those in the as-received salt. This phenomenon occurs because Ni^{2+} and

Fe^{2+} ions, introduced during FLiNaK purification, are consumed during the corrosion test via the following reactions [14, 19]:

$Ni^{2+} + Cr = Cr^{2+} + Ni$ ($\Delta G_{700}^{\circ} < 0$)
$Fe^{2+} + Cr = Cr^{2+} + Fe$ ($\Delta G_{700}^{\circ} < 0$)

The reaction products Fe and Ni deposited on the surface of the metallic Cr. Additionally, because this was a static corrosion test, the Cr corrosion product in the FLiNaK salt was not distributed evenly, particularly at the contact area between the FLiNaK salt and the metallic Cr. The Cr concentration was higher in the zone near the metallic Cr, where some green products were observed at the salt-Cr interface.

Since XANES spectroscopy is sensitive to changes in the Cr coordination environment, it was employed to determine the true oxidation state of Cr in the FLiNaK salt after corrosion testing. Figure 3 shows the Cr K-edge XANES spectra of the post-experiment FLiNaK salt and reference compounds (CrF_3, 99.98%, and CrF_2, 99%). Absorption edge shifts to higher energy as the oxidation state of the material increases [20]. Based on the edge position of the XANES spectra, it is clear that the edge position of the post-experiment FLiNaK salt, located at 6005 eV, agrees well with that of CrF_3. This indicates that the main oxidation state of Cr in FLiNaK salt is Cr^{3+}. It is known that FLiNaK salt is a strong Lewis basic solvent, and Cr^{2+} is not stable in molten FLiNaK salt [6, 21]. In the FLiNaK salt environment, the low oxidation ion Cr^{2+} would disproportionate according to the following reaction [21, 22]:

$3Cr^{2+} = 2Cr^{3+} + Cr$

The alkali metal fluorides comprising FLiNaK salt are ionic compounds, and the molten salt can easily donate F^-. In molten FLiNaK salt, the Cr^{3+} ion would interact with F^- to form complexes, which decreases the thermodynamic activity and stabilizes Cr^{3+} [6, 14, 22].

The morphology and crystal structure of the post-experiment FLiNaK salt were characterized by TEM. As depicted in Fig. 4(a), black, irregular solid particles and rod-like crystals are clearly visible in the typical TEM image. According to EDS analysis, the rod-like crystals correspond to the FLiNaK salt, whereas the black irregular particles contain Cr. Figure 4(b) presents the EDS spectrum of the black particle, showing peaks only for the elements F, Na, K, Cr, C, and Cu. Since C and Cu originate from the carbon-coated copper TEM grid, the EDS results indicate that the black particles are rich in F, Na, K, and Cr, corresponding to Cr corrosion products. To determine the structure, the Cr-rich particles (black, irregular particles) were characterized by selected area electron diffraction (SAED), as shown in Fig. 4(a). The lattice distances calculated from the diffraction dots are 4.76 Å (111), 2.88 Å (220), 2.45 Å (311), 2.40 Å (222), 1.83 Å (420), and 1.44 Å (440), which can be indexed to the standard face-centered cubic K_2NaCrF_6 structure (Table 2). Silicon single crystals with a (100) crystalline plane were used for calibration. Combined with the EDS results, this confirms that the Cr-rich black particle in the FLiNaK salt is K_2NaCrF_6.

The lattice constant was calculated to be 8.21 Å, which corresponds closely to the standard lattice constant of K_2NaCrF_6 (a = 8.27 Å, space group symmetry Fm3m, JCPDS No.: 73-0415).

To further confirm the nature of the Cr corrosion product, XRD was used to determine the structure of the salt after the corrosion test. Due to the low concentration of Cr in the post-experiment salt, the Cr corrosion products were difficult to detect by XRD. Fortunately, some green product precipitates were observed at the salt-Cr interface. The post-experiment salt containing the green product was characterized by XRD, as shown in Fig. 5. Compared to the XRD patterns of pure FLiNaK salt, some new diffraction peaks appear in the post-experiment FLiNaK salt. Although these new peaks are broad and weak due to the low concentration of the corrosion product, their positions correspond closely to the diffraction peaks of K_2NaCrF_6. The calculated d-spacing values and corresponding Miller indices are given in Table 2. These values match well with the standard diffraction patterns of K_2NaCrF_6. The new peaks can be indexed to the face-centered cubic structure K_2NaCrF_6 (JCPDS No.: 73-0415).

Comparing Fig. 5(a) with Fig. 5(b), it can be seen that the diffraction peaks of the FLiNaK salt after the corrosion test are broader than their counterparts for the salt before the corrosion test. According to the Bragg equation, this indicates that the interlayer distance of the salt increased after the corrosion test. Since the Cr atomic radius is larger than that of K and Na, the lattice parameters of the FLiNaK salt increase slightly when Cr dissolves into the salt. The XRD results are in good agreement with those obtained from SAED and EDS analyses, further verifying that the corrosion product of Cr in FLiNaK salt is K_2NaCrF_6.

As described above, the corrosion product of Cr in cooled FLiNaK salt is confirmed to be K_2NaCrF_6. The corrosion reaction in molten FLiNaK salt can be reasonably expected to satisfy the following equation:

$$CrF_3 + 2KF + NaF = K_2NaCrF_6$$

In addition, since FLiNaK salt used as reactor coolant operates under high-temperature molten conditions, future studies should consider whether the structure of Cr in high-temperature molten FLiNaK salt is consistent with that in cooled FLiNaK salt.

IV. Conclusion

In summary, pure metallic Cr was exposed to molten FLiNaK salt in a graphite crucible at 700 °C for 200 h. Due to Cr dissolution, the color of the FLiNaK salt changed from white to black-green after the corrosion test. XANES spectra revealed that the predominant oxidation state of Cr in FLiNaK salt is Cr^{3+}. Detailed structural characterization confirmed that the main corrosion product of Cr in cooled FLiNaK salt is K_2NaCrF_6. Based on indexing of the SAED and XRD patterns, the Cr corrosion product appears to be a face-centered cubic

structure with a lattice constant of a 8.21 Å.

References

[1] Rosenthal M, Haubenreich P and Briggs R. The development status of molten-salt breeder reactors. ORNL-4812. Oak Ridge, Tennessee, USA, 1972.
[2] Rosenthal M, Kasten P and Briggs R. Molten salt reactors–history, status, and potential. Nucl Appl Technol, 1970, 8: 107–117.
[3] Serp J, Allibert M, Beneš O, et al. The molten salt reactor (MSR) in generation IV: Overview and perspectives. Prog Nucl Energy, 2014, 77: 308–319. DOI: 10.1016/j.pnucene.2014.02.014
[4] Cai J, Xia X B, Chen K, et al. Analysis on reactivity initiated transient from control rod failure events of a molten salt reactor. Nucl Sci Tech, 2014, 25: 030602. DOI: 10.13538/j.1001-8042/nst.25.030602
[5] Williams D F. Assessment of candidate molten salt coolants for the NGNP/NHI Heat-Transfer Loop, in: ORNL/TM-2006/69. Oak Ridge, Tennessee, USA, 2006.
[6] Olson L C, Ambrosek J W, Sridharan K, et al. Materials corrosion in molten LiF-NaF-KF salt. J Fluorine Chem, 2009, 130: 67–73. DOI: 10.1016/j.jfluchem.2008.05.008
[7] Ouyang F Y, Chang C H, You B C, et al. Effect of moisture on corrosion of Ni-based alloys in molten alkali fluoride FLiNaK salt environments. J Nucl Mater, 2013, 437: 201–207. DOI: 10.1016/j.jnucmat.2013.02.021
[8] Ouyang F Y, Chang C H and Kai J J. Long-term corrosion behaviors of Hastelloy-N and Hastelloy-B3 in moisture-containing molten FLiNaK salt environments. J Nucl Mater, 2014, 446: 81–89. DOI: 10.1016/j.jnucmat.2013.11.045
[9] Kondo M, Nagasaka T, Tsisar V, et al. Corrosion of reduced activation ferritic martensitic steel JLF-1 in purified Flinak at static and flowing conditions. Fusion Eng Des, 2010, 85: 1430–1436. DOI: 10.1016/j.fusengdes.2010.03.064
[10] Kondo M, Nagasaka T, Xu Q, et al. Corrosion characteristics of reduced activation ferritic steel, JLF-1 (8.92Cr-2W) in molten salts Flibe and Flinak. Fusion Eng Des, 2009, 84: 1081–1085. DOI: 10.1016/j.fusengdes.2009.02.046
[11] Liu M, Zheng J, Lu Y, et al. Investigation on corrosion behavior of Ni-based alloys in molten fluoride salt using synchrotron radiation techniques. J Nucl Mater, 2013, 440: 124–128. DOI: 10.1016/j.jnucmat.2013.04.056
[12] Sellers R S, Cheng W J, Kelleher B C, et al. Corrosion of 316L Steel Alloy and Hastelloy-N Superalloy in molten Eutectic LiF-NaF-KF Salt and interaction with Graphite. Nucl Technol, 2014, 188: 192–199. DOI: 10.13182/NT13-95
[13] Qiu J, Zou Y, Yu G, et al. Compatibility of container materials with Cr in molten FLiNaK salt. J Fluorine Chem, 2014, 168: 69–74. DOI: 10.1016/j.jfluchem.2014.09.010
[14] Williams D F, Toth L M and Clarno K T. Assessment of candidate molten salt coolants for the advanced high temperature reactor (AHTR), in: ORNL/TM-2006/12. Oak Ridge, Tennessee, USA, 2006.
[15] Koger J W. Corrosion and mass transfer characteristics of $NaBF_4$–NaF (92mol%–8mol%) in Hastelloy N. Oak Ridge National Laboratory, ORNL-TM-

3866. Oak Ridge, Tennessee, USA, 1972.
[16] Briant R C, Buck J H and Miller A J, Aircraft nuclear propulsion project quarterly progress report. Oak Ridge National Laboratory, ORNL-1294. Oak Ridge, Tennessee, USA, 1952.
[17] Grimes W R. Molten-salt reactor chemistry. Nucl Technol, 1970, 8: 137-155.
[18] Yu H S, Wei X J, Li J, et al. The XAFS beamline of SSRF. Nucl Sci Tech, 2015, 5: 050102. DOI: 10.13538/j.1001-8042/nst.26.050102
[19] Olson L C. Materials corrosion in molten LiF-NaF-KF eutectic salt. Ph.D. Thesis, University of Wisconsin-Madison, 2009.
[20] Wong J, Lytle F, Messmer R, et al. K-edge absorption spectra of selected vanadium compounds. Phys Rev B, 1984, 30: 5596-5610. DOI: 10.1103/PhysRevB.30.5596
[21] Jordan W H, Cromer S J, Strough R I, et al. Aircraft nuclear propulsion project quarterly progress report. Oak Ridge National Laboratory, ORNL-1896. Oak Ridge, Tennessee, USA, 1955.
[22] Sohal M S, Ebner M A, Sabharwall P, et al. Engineering database of liquid salt thermophysical and thermochemical properties. Idaho National Laboratory, INL/EXT-10-18297. Idaho Falls, Idaho, USA, 2010.

Figures

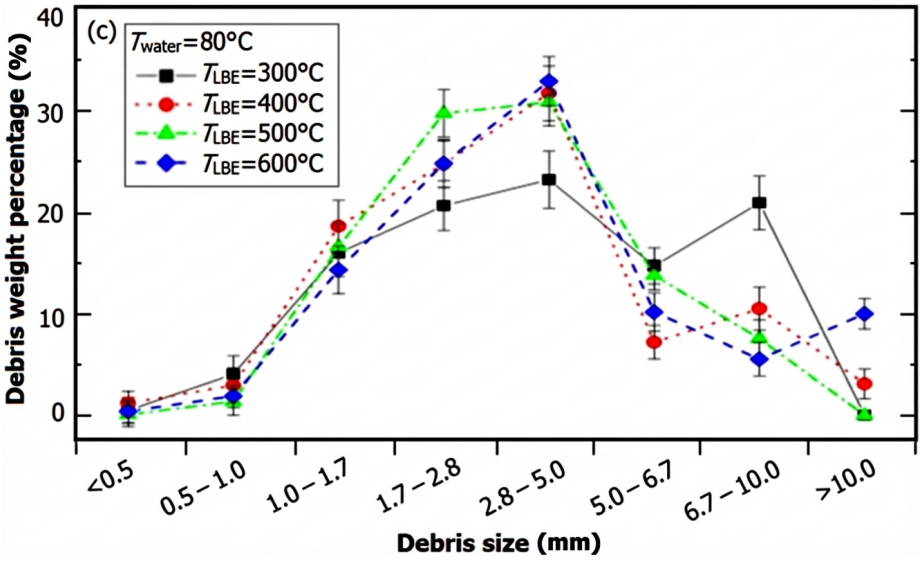

Figure 1: Figure 2

Source: ChinaXiv —Machine translation. Verify with original.